Numerical studies on piezoelectric energy harvesting from vortex-induced vibrations considering cross-wise and in-line oscillations

Lucas Oliveira Bunzel, Guilherme Rosa Franzini
Offshore Mechanics Laboratory - LMO, Escola Politécnica, University of São Paulo, Brazil

Summary. This paper presents numerical studies on piezoelectric energy harvesting from vortex-induced vibrations. The rigid cylinder is elastically supported and oscillates in both in-line and cross-wise directions. Hydrodynamic loads are modeled through nonlinear equations coupled to structural ones. Constitutive equations allow to obtain electric tension from in-line and cross-wise oscillations independently. A sensitivity study is carried out with respect to two parameters that govern the dynamics of the solid-fluid-electric system. It is showed a marked dependence of the harvested electrical power with respect to this parameter.

Introduction

Vortex-induced vibrations phenomenon (VIV) is a particular class of fluid-structure interaction problem that leads to self-excited and self-limited oscillations. Contrary to other flow-induced vibrations phenomena, VIV occurs within a limited range of free-stream velocities and present a well defined maximum oscillation amplitude. References [1] and [2] are examples of surveys on the theme. In offshore engineering scenario, VIV may be important on the prediction of lifespan of slender structures such as risers due to structural fatigue.

Even tough flow-induced vibrations produce undesirable effects on several structures, recently a series of investigations have being carried out focusing on energy harvesting these oscillations. Examples of different ways to convert part of the kinetic energy into another kind of energy are through electromagnetic effects, piezoelectricity (see [3]) or by moving wheights ([4]).

There are several investigations that focus on energy harvesting from galloping and flutter phenomena (see, for examples, references [6], [7] and [8]). VIV is also focus of investigation in this mentioned theme as can be found, for example, in references [9], [11], [12] and [13].

The present work intends to contribute with the analysis of energy harvesting from VIV considering piezoelectric effects. Particularly, focus is put on the case in which a rigid cylinder is mounted on an elastic support free to oscillate in both in-line and cross-wise directions (2-dof VIV). Herein, hydrodynamic loads were modeled by means of nonlinear equations, following the model presented in [14] and each direction is associated with a piezoelectric harvester circuit. The focus here is to present the mathematical model and the first results of a series of investigations that are being carried out at LMO. Special focus is put on the influence of two parameters of the mathematical model on the cylinder response and on the harvested electric power. Finally, it is important to emphasize that, at least to the authors knowledge, there is no investigation focusing on piezoelectric energy harvesting from 2-dof VIV.

Mathematical model

This paper focuses on energy harvesting from 2-dof VIV. A rigid cylinder with mass m_s, diameter D and length $L = 1$ is assembled to an elastic support defined by linear springs and dashpots in both cross-wise and in-line directions (indicated, respectively, by subscripts x and y). The cylinder is immersed on a fluid with density ρ. The springs present stiffness constants k_x and k_y and the dashpots are characterized by their constants c_x and c_y. Both directions have theirs own piezoelectric harvester circuits, herein assumed to be identical and defined by their capacitances C_P, electric resistance R and electromechanical coupling term θ. Figure 1 sketches the problem herein investigated.

There are some approaches employed in modeling the hydrodynamic load due to VIV. In this paper, focus is put on the so called phenomenological models. Such models employ non-linear equations (tipically, a van der Pol equation) representing the fluid dynamics. The equation representative of the fluid is coupled to a structural oscillator. Details regarding phenomenological models for VIV can be found, for example, in [15] and [16].

Herein, 2-dof VIV was modeled following the dimensionless equations presented in [14]. Displacements are normalized

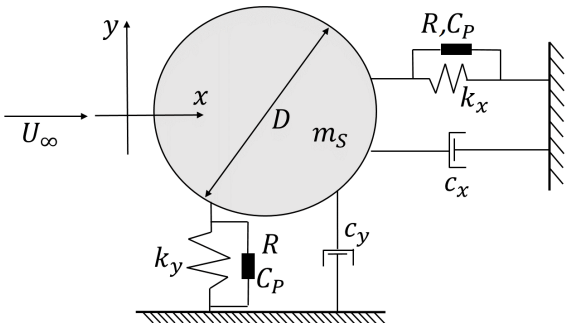

Figure 1: Schematic representation.

by the diameter D. $\dot{(\,)}$ indicates the derivative with respect to the dimensionless time $\tau = \omega_{sy}t$, being $\omega_{sy} = \sqrt{\frac{k_y}{m_t}} = \sqrt{\frac{k_y}{m_s+m_f}}$ the structural angular natural frequency in cross-wise direction. It is important to emphasize that the definition of the cross-wise natural frequency includes the potential added mass $m_f = C_a\rho\pi D^2 L/4$. In this paper, the added mass coefficient is taken as $C_a = 1$.

Piezoelectric coupling terms were considered following the approach presented in [11] for 1-dof VIV. As already mentioned, the present investigation focuses on the case in which electric energy can be harvested simultaneously from in-line and cross-wise oscillations. Following what was proposed in [15], an acceleration coupling is adopted aiming at to describe the fluid-solid interaction.

The dimensionless mathematical model is fully described by Eqs 1-6. Eqs. 1 and 2 refer, respectively, to the structural oscillations in in-line and cross-wise directions. Notice that the structural model contains cubic nonlinearities. The fluid dynamics present quadratic nonlinearities and are governed by Eqs. 3 and 4. Finally, Eqs. 5 and 6 relate the dimensionless electric tension in in-line ($V_x^* = V_x/V_0$) and cross-wise ($V_y^* = V_y/V_0$) directions with the corresponding velocities $\dot{A}_x$ and $\dot{A}_y$, being $V_0 = \frac{m_t\omega_{sy}^2 D}{\theta_y}$ a reference electric tension.

$$\ddot{A}_x + \lambda_x\dot{A}_x + {f^*}^2(A_x + \alpha_x A_x^3 + \beta_x A_x A_y^2) - M_D\Omega^2 q_x - \frac{2\pi M_L\Omega^2 q_y\dot{A}_y}{U_r} - V_x^* = 0 \tag{1}$$

$$\ddot{A}_y + \lambda_y\dot{A}_y + A_y + \alpha_y A_y^3 + \beta_y A_y A_x^2 - M_L\Omega^2 q_y + \frac{2\pi M_D\Omega^2 q_x\dot{A}_y}{U_r} - V_y^* = 0 \tag{2}$$

$$\ddot{q}_x + 2\epsilon_x\Omega(q_x^2 - 1)\dot{q}_x + 4\Omega^2 q_x - \Gamma_x\ddot{A}_x = 0 \tag{3}$$

$$\ddot{q}_y + \epsilon_y\Omega(q_y^2 - 1)\dot{q}_y + \Omega^2 q_y - \Gamma_y\ddot{A}_y = 0 \tag{4}$$

$$\dot{V}_x^* + \sigma_2 V_x^* + \sigma_1\dot{A}_x = 0 \tag{5}$$

$$\dot{V}_y^* + \sigma_2 V_y^* + \sigma_1\dot{A}_y = 0 \tag{6}$$

In Eqs. 1-4, U_r is the reduced velocity, f^* and Ω refer, respectively to the ratio between in-line and cross-wise structural natural frequencies and to the ratio between the vortex-shedding frequency ω_f and the cross-wise natural frequency. Dimensionless quantities λ_x and λ_y are related to the total damping on the model. M_D and M_L parameters that consider the oscillatory parts of lift and drag forces observed for stationary cylinders (C_L^0 and C_D^0 respectively). These parameters are written as:

$$U_r = \frac{2\pi U}{\omega_{sy}D}; f^* = \frac{\omega_{sx}}{\omega_{sy}}; \Omega = \frac{\omega_f}{\omega_{sy}} = \frac{2\pi USt}{D\omega_{sy}} = StU_r; \lambda_x = 2\zeta_x f^* + \frac{\gamma\Omega\rho D^2 L}{m_t}$$

$$\lambda_y = 2\zeta_y + \frac{\gamma\Omega\rho D^2 L}{m_t}; M_D = \frac{C_D^0}{2}\frac{\rho D^2 L}{8\pi^2 St^2 m_t}; M_L = \frac{C_L^0}{2}\frac{\rho D^2 L}{8\pi^2 St^2 m_t}; \gamma = \frac{\overline{C_D}}{4\pi St}$$

where ζ_x and ζ_y are the damping ratio in in-line and cross-wise directions, St is the Strouhal number, γ is the stall parameter and $\overline{C_D}$ is the mean drag coefficient for the the stationary cylinder. Parameter ϵ_y was adopted following the empirical expression presented in [14]. This mentioned expression is given by Eq. 7 and takes into account the influence of the mass ratio parameter $m^* = 4m_s/\rho\pi D^2 L$.

$$\epsilon_y = 0.00234e^{0.228m^*} \tag{7}$$

Dimensionless quantities σ_1 and σ_2 are related to the piezoelectric harvested circuits. These quantities depend on the electrical resistance, the capacitance and the electromechanical coupling term associated to the electric circuits. Mathematically:

$$\sigma_1 = \frac{\theta^2}{m_t\omega_{sy}^2 C_P}; \sigma_2 = \frac{1}{\omega_{sy}RC_P} \tag{8}$$

Some investigations such as, for example, reference [12], discuss energy harvesting considering the power dissipated at the dashpot. In this present investigation, focus is put on the electrical power dissipated at the cross-wise circuit (P_{el}). Such power is made dimensionless with respect to the flux of kinetic energy across the cylinder's front area as:

$$\eta = \frac{P_{el}}{1/2\rho U_\infty^3 DL} = \frac{2V_y^2}{R_y\rho U^3 D} = \frac{4\pi^4}{U_r^3}\frac{\sigma_{2,y}}{\sigma_{1,y}}(C_a + m^*)(V_y^*)^2 \tag{9}$$

Notice that η can be interpreted as the piezoelectric energy harvesting efficiency. In this paper, focus is put on $\bar{\eta}$, i.e., the time-averaged values of $\bar{\eta}$ during the steady-state response.

Eqs 1-6 are numerically integrated using MATLAB® ode45 function (Runge-Kutta scheme). The total simulation time is $\tau_{max} = 200$ and the time-step is constant and equal to $\Delta\tau = 0.01$. Two non-trivial initial conditions were adopted, namely $q_x(0) = q_y(0) = 0.2$.

Results

This paper focuses on the influence of both σ_1 and f^* on the energy harvesting. Even though the properties of the electric circuit can be different in the two directions, herein they are assumed to be equal and the corresponding subscript will be suppressed.

The inertial and geometrical properties of the cylinder are the same experimentally tested in a recirculating water channel facility by [17]. In this mentioned investigation, $D = 44.45\text{mm}, f_{sy} = 0.69\text{Hz}, L/D = 13, m^* = 2.6, f^* = 1, \zeta_x = \zeta_y = 0.0007$ and $\rho = 1000\text{kg/m}$. Following what was used in [11], the capacitance and the electric resistance of the piezoelectric harvesters are, respectively, 120nF and 5kΩ, leading to $\sigma_2 = 384$. Following the suggestion presented in [15], an amplified mean drag coefficient $\overline{C_D} = 2$ is considered together with $St = 0.20$. These values lead to $\gamma = 0.8$ for all values of U_r. Tab. 1 presents others parameters of the wake-oscillator model presented in [14] and herein adopted.

Table 1: Parameters from Zanganeh and Srinil's phenomenological model.

Parameter	Value	Parameter	Value	Parameter	Value
ϵ_x	0.3	$\Gamma_x = \Gamma_y$	12	C_L^0	0.3
$\alpha_x = \alpha_y$	0.7	$\beta_x = \beta_y$	0.7	C_D^0	0.2

Firstly, we compare the numerical results obtained from the wake-oscillator model for pure VIV (i.e., when the electromechanical coupling term is null or, equivalently, when $\sigma_1 = 0$) and $f^* = 1$ with those experimentaly obtained and presented in [17].

The numerical-experimental comparison of oscillation amplitudes is presented in Fig. 2. Both qualitative and quantitative agreements are found in this mentioned correlation. Even though the numerical in-line oscillation amplitudes are smaller than the experimental results (Fig. 2(a)), a marked adherence is found for the results concerning cross-wise direction - see Fig. 2(b).

Notice that in the range $8 < U_r < 10$, the experimental data reveals characteristics of the lower branch of response, following the nomeclature adopted by [18]. On the other hand, the numerical results obtained using the wake-oscillator model do not capture this feature. This is a well-known aspect of this kind of mathematical model that are being pursued by the research group. A possible way to reach a better adherence in the lower branch is to adopt a different set o parameters for the wake-oscillator model for this range of reduced velocity, similarly to what was carried out in [19] for 1-dof VIV. Even though the importance of a better capture of the lower branch, this is left for a further work.

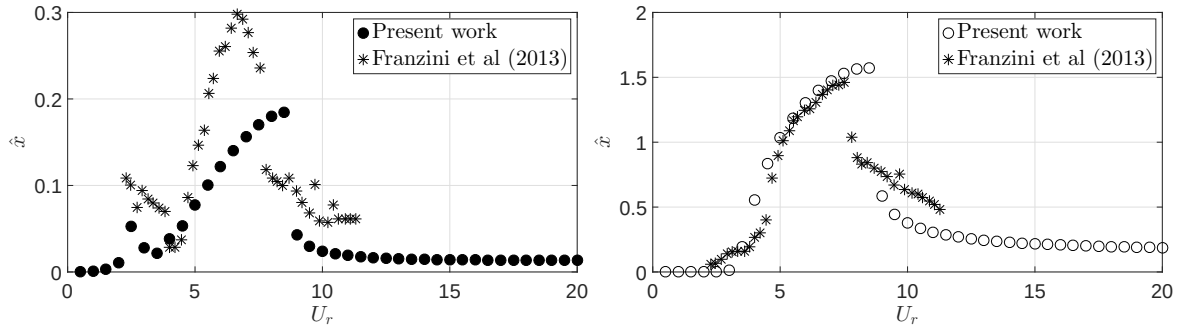

(a) In-line oscillation amplitude. (b) Cross-wise oscillation amplitude.

Figure 2: Numerical-experimental comparison. $f^* = 1$ and $\sigma_1 = 0$.

Fig. 3 illustrates a trajectory in the xy plane and clearly reveals a well know feature of 2-dof VIV, namely the presence of "eight-shapped" trajectories. This mentioned plot indicates the classical relation between dominant frequencies $f_{d,x}/f_{d,y} = 2$.

The results presented in this Subsection indicate that the wake-oscillator model herein adopted is representative of 2-dof VIV phenomenon. In this scenario, we now discuss the results obtained when the piezoelectric effect is concomitant to VIV.

The first aspect to be investigated in this new scenario is the influence of σ_1 on the cylinder. Physically, σ_1 is varied by changing the electromechanical coupling term. As already mentioned, $\sigma_2 = 384$ is adopted. Finally, the in-line to cross-wise natural frequency ratio is $f^* = 1$. For the sake of clearity of this analysis herein presented, considering $\theta = 0.00155\text{N/V}$ as in [11], it is obtained $\sigma_1 = 0.33$. In this Subsection, this mentioned value, as well as two orders of magnitude above and one order of magnitude below are studied.

Fig. 4 presents the oscillation amplitudes, the maximum electric tension and the energy harvesting efficiency as functions of the reduced velocity. It is clearly noticeable that the oscillation amplitudes in in-line and cross-wise directions are practically not affected by the piezoelectric effect for $\sigma_1 = 0.033, 0.33$ and 3.3 (see Figs. 4(a) and 4(b)). On the other

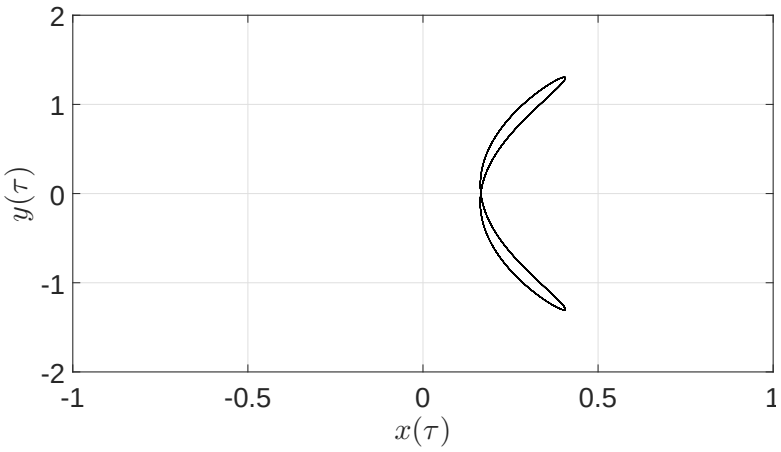

Figure 3: Trajectories in the xy plane. Numerical results with $f^* = 1$.

hand, for $\sigma_1 = 33$, it is observed an important decrease in both in-line and cross-wise oscillation amplitudes. Still considering the oscillation amplitudes plots, the piezoelectric effect is irrelevant for $U_r > 10$, i.e., in the onset of the desynchronization between vortex-shedding and oscillations.

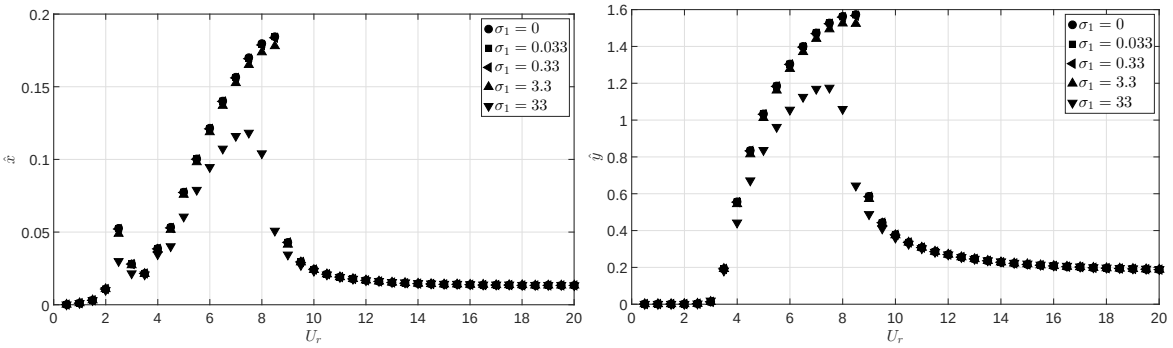

(a) In-line oscillation amplitude.

(b) Cross-wise oscillation amplitude.

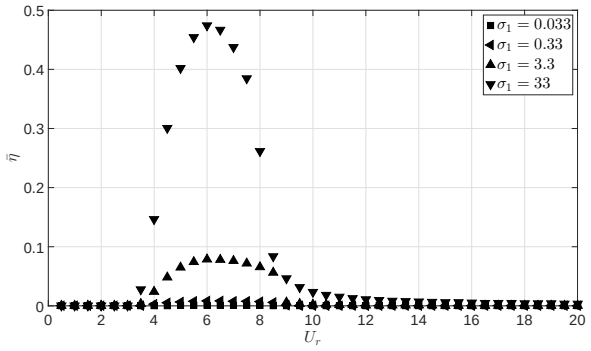

(c) Time-averaged energy harvesting efficiency.

Figure 4: Influence of σ_1 on the cylinder's response and harvested power - numerical results.

The time-averaged energy harvesting efficiency as functions of the reduced velocity are presented in Fig. 4(c). As expected, the larger the dimensionless quantity σ_1, the larger is the value of $\bar{\eta}$ for a given reduced velocity. Not surprising, energy harvesting is possible only in the interval $4 < U_r < 8$, i.e., in the range of reduced velocities in which the lock-in is observed and that presents significant oscillation amplitudes. This mentioned plot also reveals that a peak of efficiency larger than 5% is only possible for $\sigma_1 = 3.3$ or $\sigma_1 = 33$.

A second set of simulations is carried out focusing the influence of the in-line to cross-wise natural frequencies ratio in the cylinder's response. While σ_1 is kept constant and equal to 3.3, three values of f^* are studied, namely $f^* = 1/2, 1$ and $f^* = 2$.

Fig. 5 presents the oscillation amplitudes and the energy harvesting efficiency as functions of the reduced velocity. As can be seen in Fig. 5(a), it is observed a marked increase in the in-line oscillation amplitudes for $f^* = 2$.

The influence of f^* on energy harvesting efficiency can be found in 5(c). This mentioned plot reveals that $\bar{\eta}$ varies from 0.06 for $f^* = 1/2$ to 0.08 for $f^* = 1$. Notice also that the peak of $\bar{\eta}$ for $f^* = 1$ is verified for a slightly value of reduced velocity.

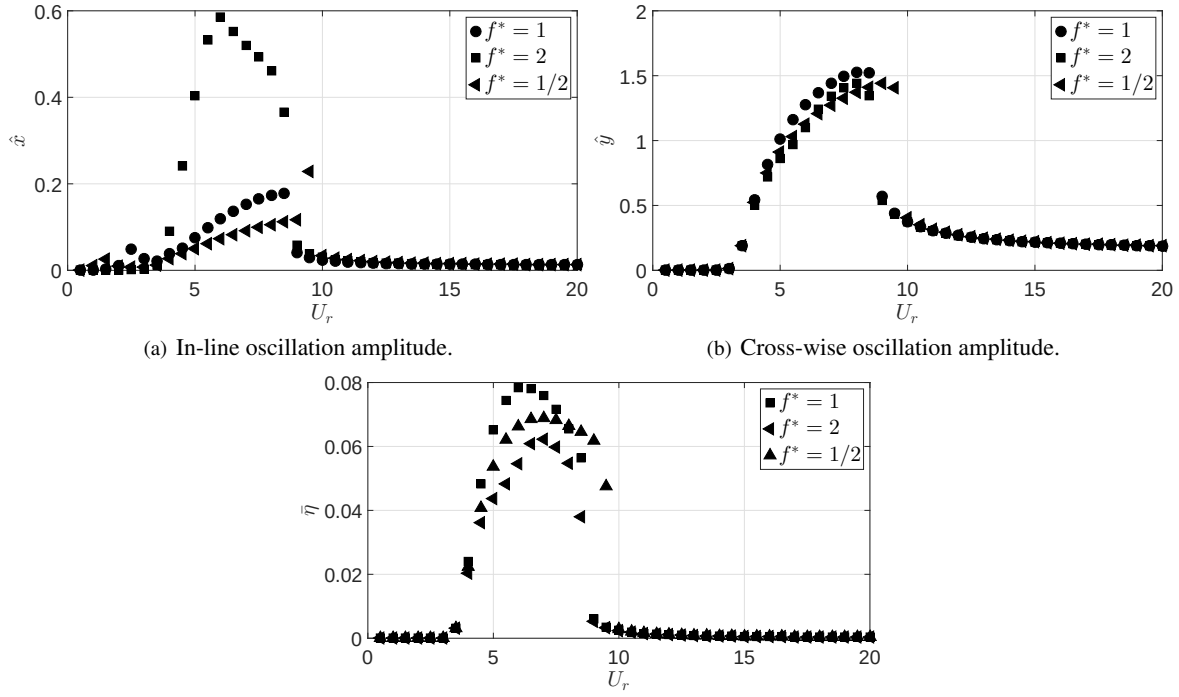

(a) In-line oscillation amplitude.

(b) Cross-wise oscillation amplitude.

(c) Time-averaged energy harvesting efficiency.

Figure 5: Influence of σ_1 on the cylinder's response and harvested power - numerical results. $\sigma_1 = 3.3$.

The last aspecto to be herein discussed is the electric power that would be harvested if the cylinder tested by [17] was fitted with piezoelectric harvesters. Herein, only the harvesters are defined by $\sigma_1 = 3.3$ and $\sigma_2 = 384$. Considering the experimental parameters already presented, the free-stream velocity can be easily calculated as $U_\infty = U_r \omega_{su} D/2\pi$. Using Eq. 9, the electrical power is obtained.

The time-averaged electrical power is plotted as a function of the free-stream velocity in Fig. 6. This mentioned plot indicates that the maximum time-averaged electric power harvested at the cross=wise piezoelectric circuit is close to $80\mathrm{mW}$.

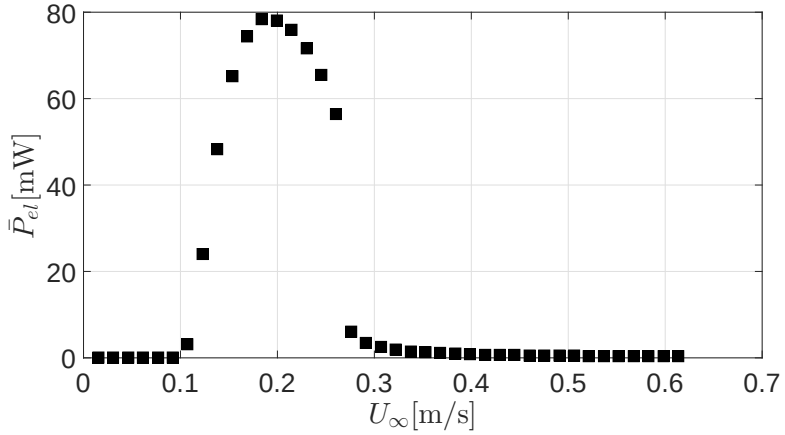

Figure 6: Variation of harvested electric power as function of free-stream velocity.

Conclusions

This paper presented the first results obtained from a series of efforts aiming at deeper analysis on energy harvesting from flow-induced vibrations phenomena. Focus was put on energy harvesting from Vortex-Induced Vibrations (VIV) of a rigid cylinder assembled to a piezoelectric elastic support that allows oscillations in the horizontal plane (2-dof VIV). Hydrodynamic loads were modeled through wake-oscillator model. At least to the author's knowledge, there is no investigation focusing on energy harvesting from 2-dof VIV.

The mathematical model was numerically integrated and oscillation amplitudes and harvested electric power were obtained as functions of the reduced velocity and different parameters related to the cylinder and the piezoelectric circuits. A large number of parameters govern the equations of motion and, hence, only two parameters were focus of the analysis. One of these parameters was the in-line to cross-wise natural frequencies ratio (f^*) and the other one is σ_1, a

dimensionless quantity related to the electromechanical coupling term of the piezoelectric circuit.
Firstly, it was showed that the wake-oscillator model is able to reproduce, both qualitatively and quantitatively, the oscillation amplitude curves for the pure VIV condition. Considering the cross-wise direction, it was found a marked adherence with experimental data for reduced velocities up to $U_r = 8$. On the other hand, the numerical results indicated oscillation amplitudes lower than experimental data for $U_r > 8$.
In a second set of analysis, the cylinder is coupled to the piezoelectric harvesters and the parameter σ_1 is varied, keeping the other parameters constant. Considering $\sigma_1 = 0.033, 0.33$ and 3.3, the energy harvesting efficiency is lower than 0.1 with practically no decrease in the oscillations amplitudes. Another aspect investigated is the influence of the in-line to cross-wise natural frequencies ratio considering $\sigma_1 = 3.3$. It was found that the maximum energy harvesting efficiency decreases from 0.08 for $f^* = 1$ to 0.06 for $f^* = 2$.
Further work include a deeper analysis of the influence of the parameters that govern the mathematical model on the harvested electric power, as well as a comparison between the piezoelectric energy harvesting from 1-dof and 2-dof VIV. It is also planned a series of studies comparing the energy harvesting efficiency from different flow-induced vibrations problems.

Acknowledgments

First author acknowledges São Paulo Research Foundation (FAPESP) for his undergraduate scholarship, grant 2014/19530-2. Second author is grateful to Brazilian National Council for Research (CNPq) and to FAPESP for the grants 310595/2015-0 and 2016/20929-2. This work is part of a research project on renewable energy from oceans supported by NAP-OS (University of São Paulo Nucleus for Research Support - Sustainable Ocean). Finally, the authors acknowledge Prof. Celso Pesce, from Escola Politécnica, University of São Paulo, for his valuable comments.

References

[1] Bearman, P. W. (2011) Circular cylinders wake and vortex-induced vibrations. *Journal of Fluids and Structures*, **v. 27.**, p.648-658.

[2] Williamson, C. H. K.; Govardhan, R. N. (2004) Vortex-Induced Vibrations. *Annual Review of Fluids Mechanics*, **v. 36.**, p.413-455.

[3] Erturk, A.; Inman, D.J. (2011) Piezoelectric energy harvesting. John Wiley & Sons.

[4] Fernandes, A.C.; Armandei, M. (2014) Low-head hydropower extraction based on torsional galloping *Renewable energy*, **v. 69**, 447-452.

[5] Tang, L.; Païdoussis, M.P.; Jiang, J. (2009) Cantilever flexible plates in axial flow: Energy transfer and the concept of flutter-mill *Journal of Sound and Vibration*,v. 326, p. 263-276

[6] Barrero-Gil, A.; Alonso, G.; Sanz-Andres, A. (2010) Energy harvesting from transverse galloping. *Journal of Sound and Vibration*, **v. 329**, p. 2873-2883.

[7] Doaré, O.; Michelin, S. (2011) Piezoelectric coupling in energy harvesting fluttering flexible plates: linear stability analysis and conversion efficiency. *Journal of Fluids and Structures*, **v. 27**, p. 1357-1375.

[8] Franzini, G.R.; Santos, R.C.S.; Pesce, C. P. (2016) Energy harvesting from transverse galloping enhanced by parametric excitation. *Proceedings of the 11th International Conference on Flow-Induced Vibration - FIV2016*.

[9] Bernitsas, M.M.; Raghavan, K.; Ben-Simos, Y.; Garcia, E. M. H. (2006) VIVACE (Vortex Induced Vibration Aquatic Clean Energy): A new concept in generation of clean and renewable energy from fluid flow. *Proceedings of OMAE2006 - International Conference on Offshore Mechanics and Artic Engineering*.

[10] Akaydin, H.D.; Elvin, N.; Andreopoulos (2012) The performance of a self-excited fluidic energy harvester *Smart Material and Structures*,**v. 21**, p. 1-13.

[11] Mehmood, A.; Abdelkefi, A.; Hajj, A. A.; Nayfeh, A. H.; Akthar, I.; Nuhait, A. O. (2013) Piezoeletric energy harvesting from vortex-induced vibrations of circular cylinder. *Journal of Sound and Vibration*, **v. 332**, p.4656-4667.

[12] Grouthier, C.; Michelin, S.; Bourguet, R.; Modarres-Sadeghi, Y.; de Langre, E. (2014) On the efficiency of energy harvesting using vortex-induced vibrations of cables. *Journal of Fluids and Structures*, **v. 49.**, p.427-440.

[13] Dai, H.L.; Abdelkefi, A.; Wang, L. (2014) Piezoelectric energy harvesting from concurrent vortex-induced vibrations and base excitation *Nonlinear Dynamics*,**v. 77**, p. 967-981.

[14] Zanganeh, H; Srinil, N. (2014) Characterization on Variable Hydrodynamic Coefficients and Maximum Responses in Two-Dimensional Vortex-Induced Vibrations With Dual Resonances. *Journal of Vibration and Acoustics*, **v. 136.**, p.051014-1-051014-15.

[15] Facchinetti, M. L.; de Langre, E.; Biolley, F. (2004) Coupling of structure and wake oscillators in vortex-induced vibrations. *Journal of Fluids and Structures*, **v. 19**, 123-140.

[16] Gabbai, R.D.; Benaroya, H. (2005) An overview of modeling and experiments of vortex-induced vibration of circular cylinders. *Journal of Sound and Vibration*, **v. 282**, p.575-616.

[17] Franzini, G.R.; Gonçalves, R.T., Meneghini, J.R., Fujarra, A.L.C. (2013) One and two degrees-of-freedom Vortex-Induced Vibration experiments with yawed cylinders. *Journal of Fluids and Structures*, **v. 42**, p.401-420.

[18] Khalak, A.; Williamson, C.H.K. (1999) Motions, forces and modes transitions in Vortex-Induced Vibration at low Reynolds number. *Journal of Fluids and Structures*, **v. 13**, p. 813-851.

[19] Ogink, R.H.M.; Metrikine, A.V. (2010) A wake oscillator with frequency dependent coupling for the modeling of vortex-induced vibration. *Journal of Sound and Vibration*,**v. 329**, p. 5452-5473.